NBS
PUBLICATIONS

# NBS TECHNICAL NOTE 1312

U.S. DEPARTMENT OF COMMERCE / National Bureau of Standards

# An Investigation of a Ray-Mode Representation of the Green's Function in a Rectangular Cavity

D.I. Wu
D.C. Chang

The National Bureau of Standards[1] was established by an act of Congress on March 3, 1901. The Bureau's overall goal is to strengthen and advance the nation's science and technology and facilitate their effective application for public benefit. To this end, the Bureau conducts research to assure international competitiveness and leadership of U.S. industry, science and technology. NBS work involves development and transfer of measurements, standards and related science and technology, in support of continually improving U.S. productivity, product quality and reliability, innovation and underlying science and engineering. The Bureau's technical work is performed by the National Measurement Laboratory, the National Engineering Laboratory, the Institute for Computer Sciences and Technology, and the Institute for Materials Science and Engineering.

## *The National Measurement Laboratory*

Provides the national system of physical and chemical measurement; coordinates the system with measurement systems of other nations and furnishes essential services leading to accurate and uniform physical and chemical measurement throughout the Nation's scientific community, industry, and commerce; provides advisory and research services to other Government agencies; conducts physical and chemical research; develops, produces, and distributes Standard Reference Materials; provides calibration services; and manages the National Standard Reference Data System. The Laboratory consists of the following centers:

- Basic Standards[2]
- Radiation Research
- Chemical Physics
- Analytical Chemistry

## *The National Engineering Laboratory*

Provides technology and technical services to the public and private sectors to address national needs and to solve national problems; conducts research in engineering and applied science in support of these efforts; builds and maintains competence in the necessary disciplines required to carry out this research and technical service; develops engineering data and measurement capabilities; provides engineering measurement traceability services; develops test methods and proposes engineering standards and code changes; develops and proposes new engineering practices; and develops and improves mechanisms to transfer results of its research to the ultimate user. The Laboratory consists of the following centers:

- Applied Mathematics
- Electronics and Electrical Engineering[2]
- Manufacturing Engineering
- Building Technology
- Fire Research
- Chemical Engineering[3]

## *The Institute for Computer Sciences and Technology*

Conducts research and provides scientific and technical services to aid Federal agencies in the selection, acquisition, application, and use of computer technology to improve effectiveness and economy in Government operations in accordance with Public Law 89-306 (40 U.S.C. 759), relevant Executive Orders, and other directives; carries out this mission by managing the Federal Information Processing Standards Program, developing Federal ADP standards guidelines, and managing Federal participation in ADP voluntary standardization activities; provides scientific and technological advisory services and assistance to Federal agencies; and provides the technical foundation for computer-related policies of the Federal Government. The Institute consists of the following divisions:

- Information Systems Engineering
- Systems and Software Technology
- Computer Security
- Systems and Network Architecture
- Advanced Computer Systems

## *The Institute for Materials Science and Engineering*

Conducts research and provides measurements, data, standards, reference materials, quantitative understanding and other technical information fundamental to the processing, structure, properties and performance of materials; addresses the scientific basis for new advanced materials technologies; plans research around cross-cutting scientific themes such as nondestructive evaluation and phase diagram development; oversees Bureau-wide technical programs in nuclear reactor radiation research and nondestructive evaluation; and broadly disseminates generic technical information resulting from its programs. The Institute consists of the following Divisions:

- Ceramics
- Fracture and Deformation[3]
- Polymers
- Metallurgy
- Reactor Radiation

[1]Headquarters and Laboratories at Gaithersburg, MD, unless otherwise noted; mailing address Gaithersburg, MD 20899.
[2]Some divisions within the center are located at Boulder, CO 80303.
[3]Located at Boulder, CO, with some elements at Gaithersburg, MD

# An Investigation of a Ray-Mode Representation of the Green's Function in a Rectangular Cavity

D.I. Wu
D.C. Chang[†]

Electromagnetic Fields Division
Center for Electronics and Electrical Engineering
National Engineering Laboratory
National Bureau of Standards
Boulder, Colorado 80303-3328

†University of Colorado
Boulder, Colorado 80309

U.S. DEPARTMENT OF COMMERCE, Clarence J. Brown, Acting Secretary

NATIONAL BUREAU OF STANDARDS, Ernest Ambler, Director

Issued September 1987

National Bureau of Standards Technical Note 1312
Natl. Bur. Stand. (U.S.), Tech Note 1312, 48 pages (Sept. 1987)
CODEN:NBTNAE

U.S. GOVERNMENT PRINTING OFFICE
WASHINGTON: 1987

For sale by the Superintendent of Documents, U.S. Government Printing Office, Washington, DC 20402

CONTENTS

Page

## FOREWORD

This report is a continuation of efforts and collaboration between the staff of the University of Colorado at Boulder and the Electromagnetic Fields Division of the National Bureau of Standards (NBS) to establish a theoretical basis for the design of a mode-stirred (reverberating) chamber. This work is a part of the doctoral dissertation work undertaken by D. I. Wu. The project was sponsored by NBS under the technical supervision of Professor David C. Chang of CU and Dr. Motohisa Kanda of NBS.

The goals of this project are to understand analytically the effect of a rotating scatterer or a stirrer in a large rectangular cavity, and to provide analytical tools usable in the design of an effective stirrer. In treating the stirrer as a scatterer, the dyadic Green's function expressed in the modal form as the kernel for the desired integral equation is encountered. Due to the cumbersome nature of the dyad, numerical computations are relied upon. However, since the convergence of the triple summation of modes embedded in the dyad is known to be impractically slow, the issue of evaluating the dyad in a numerically efficient manner arises. This prompts our search for an alternate representation for the dyad which would allow feasible numerical computation.

This report describes in detail the analytical methods used in obtaining an efficient hybrid representation for the dyad. The effectiveness of this hybrid representation is also illustrated in this report. With this hybrid representation, any numerical computation involving the dyad can now be carried out in a feasible manner.

Previous publications under the same effort include:

Tippet, J. C.; Chang, D. C. Radiation characteristics of dipoles sources located inside a rectangular coaxial transmission line. Nat. Bur. Stand. (U.S.) NBSIR 75-829; 1976 January.

Tippet, J. C.; Chang, D. C.; Crawford, M. L. An analytical and experimental determination of the cut-off frequencies of higher-order TE modes in a TEM cell. Nat. Bur. Stand. (U.S.) NBSIR 76-841; 1976 June.

Tippet, J. C.; Chang, D. C. Higher-order modes in rectangular coaxial line with infinitely thin inner conductor. Nat. Bur. Stand. (U.S.) NBSIR 78-873; 1978 March.

Sreenivasiah, I.; Chang, D. C. A variational expression for the scattering matrix of a coaxial line step discontinuity and its application to an over moded coaxial TEM cell. Nat. Bur. Stand. (U.S.) NBSIR 79-1606; 1979 May.

Tippet, J. C.; Chang, D. C. Dispersion and attenuation characteristics of modes in a TEM cell with a lossy dielectric slab. Nat. Bur. Stand. (U.S.) NBSIR 79-1615; 1979 August.

Sreenivasiah, I.; Chang, D. C.; Ma, M. T. Characterization of electrically small radiating sources by tests inside a transmission line cell. Nat. Bur. Stand. (U.S.) Tech. Note 1017; 1980 February.

Wilson, P. F.; Chang, D. C.; Ma, M. T. Excitation of a TEM cell by a vertical electric Hertzian dipole. Nat. Bur. Stand. (U.S.) Tech Note 1037; 1981 March.

Sreenivasiah, I.; Chang, D. C.; Ma, M. T. A method of determining the emission and susceptibility levels of electrically small objects using a TEM cell. Nat. Bur. Stand. (U.S.) Tech. Note 1040; 1981 April.

Wilson, P. F.; Chang, D. C; Ma, M. T. Input impedance of a probe antenna exciting a TEM cell. Nat Bur. Stand. (U.S.) Tech. Note 1054; 1982 April.

Liu, B. H.; Chang, D. C.; Ma, M. T. Eigenmodes and the composite quality factor of a reverberating chamber. Nat. Bur. Stand. (U.S.) Tech. Note 1066; 1983 August.

An Investigation of a Ray-Mode Representation of the Green's Function in a Rectangular Cavity

D. I. Wu and D. C. Chang*

Electromagnetic Fields Division
National Bureau of Standards
Boulder, Colorado 80303

It is well known that a point-source excited field in a rectangular cavity can be represented either in terms of summation of modes or in terms of rays produced by the equivalent image sources. Both representations involve series that are slowly convergent; so computation of fields inside the cavity is difficult. To obtain a numerically efficient scheme, a hybrid ray-mode representation is developed here using the finite Poisson summation formula. The modal representation is modified in such a way that all the modes near resonance are retained while the truncated remainder of the mode series is expressed in terms of a weighted contribution of rays. For a large cavity, the contribution of rays from far-away images becomes small; therefore the ray sum can be approximated by one or two dominant terms without a loss of numerical accuracy. To illustrate the accuracy and the computational simplification of this ray-mode representation, numerical examples are included with the conventional mode series (summed at the expense of long computation time) serving as a reference.

Key words: Green's function; hybrid representation; modal representation; Poissòn summation formula; ray-mode representation; rectangular cavity.

## 1. Introduction

In analyzing fields due to scattering or excitation of a radiating structure inside an electrically large and over-moded rectangular cavity such as the NBS reverberating chamber used in EMI testing[1,2], we often encounter the dyadic Green's function expressed in the modal form as the kernel for the desired integral equation. One issue that often arises is how to obtain a numerically efficient scheme for computing the dyad, particularly when the observation point is close to the source point. The

*Department of Electrical Engineering, University of Colorado, Boulder, CO 80309.

use of modal representation is clearly not practical, since the convergence of the triple infinite sum of higher-order, nonresonant modes is notoriously, if not impractically, slow.

In this report, a finite, three-dimensional Poisson summation formula is utilized to obtain a hybrid representation for the Green's function. This hybrid representation consists of two terms. The first term, called the mode sum, consists of a finite number of modes near resonance. The number of modes varies depending upon the summation bandwidth chosen. The second term, referred to as the ray sum, consists of all the images produced by the reflecting boundaries of the cavity. The bandwidth for the mode sum is a mathematical quantity. A balancing effect exists between the two terms in that as the bandwidth increases, the contribution from the mode sum increases while the contribution from the ray sum decreases. Though the bandwidth is an arbitrary quantity, it does have a minimal requirement. Below this minimal value the hybrid representation becomes a poor approximation to the modal representation. As will be shown, this minimal requirement stems from the approximation involved in transforming from the rectangular coordinates to spherical coordinates in applying the finite Poisson summation formulation.

This hybrid representation is especially effective when the source point is close to the observation point. For a large cavity, oftentimes the second or the third layer images and beyond are far away from the observation point; so the contribution from these images becomes very small. Therefore, for the ray sum, we found that it is often sufficient to keep just the self term and perhaps several adjacent images to obtain the desired numerical accuracy.

## 2. Dyadic Green's Function

Consider a rectangular cavity with a perfectly conducting scatterer as shown in figure 1. Fields incident on the scatterer induce a current $\vec{J}$ on the surface of the scatterer, which in turn re-radiates fields inside the cavity. The re-radiated or scattered fields can be expanded using two types of orthogonal basis functions, of which one has a zero divergence and the other a zero curl[3].

$$\vec{E}^{s} = \sum_{\alpha=(m,n,p)=0}^{\infty} \sum \sum \left\{ p_{\alpha}^{TE} \vec{E}_{\alpha}^{TE} + p_{\alpha}^{TM} \vec{E}_{\alpha}^{TM} + q_{\alpha} \vec{F}_{\alpha} \right\}, \tag{1}$$

where

$$\nabla \cdot \vec{E}_{\alpha}^{TE} = \nabla \cdot \vec{E}_{\alpha}^{TM} = 0; \quad \nabla \times \vec{F}_{\alpha} = 0. \tag{1a}$$

If we define TE and TM with respect to the $\hat{z}$-axis, the modal fields $\vec{E}_{\alpha}^{TE}$, $\vec{E}_{\alpha}^{TM}$, and $\vec{F}_{\alpha}$ can be found using boundary conditions,

$$\vec{E}_{\alpha}^{TE} = \nabla \times \frac{\epsilon_{\alpha}}{\sqrt{abc}} \cos(\frac{m\pi}{a} x)\cos(\frac{n\pi}{b} y)\sin(\frac{p\pi}{c} z) \; \hat{z},$$

$$\vec{E}_{\alpha}^{TM} = \nabla \times \nabla \times \frac{\epsilon_{\alpha}}{\sqrt{abc}} \sin(\frac{m\pi}{a} x)\sin(\frac{n\pi}{b} y)\cos(\frac{p\pi}{c} z) \; \hat{z},$$

$$\vec{F}_{\alpha} = \nabla \left\{ \frac{\epsilon_{\alpha}}{\sqrt{abc}} \sin(\frac{m\pi}{a} x)\sin(\frac{n\pi}{b} y)\sin(\frac{p\pi}{c} z) \right\}, \tag{2}$$

$$\epsilon_{\alpha} = \begin{cases} 2 & \text{for } m=0, \text{ or } n=0, \text{ or } p=0 \\ \sqrt{8} & \text{for } m,n,p \neq 0. \end{cases}$$

The modal coefficients $p_{\alpha}^{TE}$, $p_{\alpha}^{TM}$, $q_{\alpha}$ can be found by substituting eq (2) into the vector wave equation and applying orthogonality conditions, and they can be expressed as[4]

$$p_\alpha^{TE} = -i\omega\mu \left(\frac{1}{k_\alpha^2 - k_o^2}\right) \frac{\langle\vec{J} \cdot \vec{E}_\alpha^{TE}\rangle}{k_{mn}^2},$$

$$p_\alpha^{TM} = -i\omega\mu \left(\frac{1}{k_\alpha^2 - k_o^2}\right) \frac{\langle\vec{J} \cdot \vec{E}_\alpha^{TM}\rangle}{k_\alpha^2 k_{mn}^2}, \tag{3}$$

and

$$q_\alpha = i\omega\mu \frac{\langle\vec{J} \cdot \vec{F}_\alpha\rangle}{k_o^2 k_\alpha^2},$$

where the time dependence is $e^{i\omega t}$, $k_o = \omega(\mu_o \epsilon_o)^{1/2}$ is the wave number of the material in the cavity space, and $k_\alpha$ and $k_{mn}$ are the normalized and the transverse cut-off frequencies of the cavity modes,

$$k_\alpha = \left[\left(\frac{m\pi}{a}\right)^2 + \left(\frac{n\pi}{b}\right)^2 + \left(\frac{p\pi}{c}\right)^2\right]^{1/2},$$

and

$$k_{mn} = \left[\left(\frac{m\pi}{a}\right)^2 + \left(\frac{n\pi}{b}\right)^2\right]^{1/2}. \tag{4}$$

The $\langle \cdot \rangle$ notation implies the integral of the dot product of the two vector functions enclosed, integrated over the surface of the scatterer.

The electric field can therefore be expressed as

$$\vec{E}^s = -i\omega\mu \langle\vec{J} \cdot \overleftrightarrow{G}\rangle, \tag{5}$$

where

$$\overleftrightarrow{G} = \sum_{\alpha=(m,n,p)=0}^{\infty} \sum \sum \left\{ \frac{\vec{E}_\alpha^{TE}(r)\vec{E}_\alpha^{TE}(r')}{(k_\alpha^2 - k_o^2)k_{mn}^2} - \frac{\vec{E}_\alpha^{TM}(r)\vec{E}_\alpha^{TM}(r')}{(k_\alpha^2 - k_o^2)k_{mn}^2 k_\alpha^2} - \frac{\vec{F}_\alpha(r)\vec{F}_\alpha(r')}{k_\alpha^2 k_o^2} \right\}. \tag{5a}$$

Rearranging terms, we can expressed the dyadic Green's function in a modal form,

$$\overleftrightarrow{G} = -\nabla\nabla' \frac{1}{k_o^2} \sum_{m=0}^{\infty} \sum_{n=0}^{\infty} \sum_{p=0}^{\infty} \frac{1}{k_\alpha^2 - k_o^2} \Phi_\alpha(r)\, \Phi_\alpha(r') \tag{6}$$

$$+ \sum_{m=0}^{\infty} \sum_{n=0}^{\infty} \sum_{p=0}^{\infty} \frac{1}{k_\alpha^2 - k_o^2} [\phi_\alpha^x(r)\phi_\alpha^x(r')\hat{x}\hat{x} + \phi_\alpha^y(r)\phi_\alpha^y(r')\hat{y}\hat{y} + \phi_\alpha^z(r)\phi_\alpha^z(r')\hat{z}\hat{z}],$$

where

$$\phi_\alpha^x (r) = \frac{\epsilon_\alpha}{\sqrt{abc}} \cos(\frac{m\pi}{a} x) \sin(\frac{n\pi}{b} y) \sin(\frac{p\pi}{c} z),$$

$$\phi_\alpha^y (r) = \frac{\epsilon_\alpha}{\sqrt{abc}} \sin(\frac{m\pi}{a} x) \cos(\frac{n\pi}{b} y) \sin(\frac{p\pi}{c} z), \tag{6a}$$

$$\phi_\alpha^z (r) = \frac{\epsilon_\alpha}{\sqrt{abc}} \sin(\frac{m\pi}{a} x) \sin(\frac{n\pi}{b} y) \cos(\frac{p\pi}{c} z),$$

and

$$\Phi_\alpha (r) = \frac{\epsilon_\alpha}{\sqrt{abc}} \sin(\frac{m\pi}{a} x) \sin(\frac{n\pi}{b} y) \sin(\frac{p\pi}{c} z).$$

The dyadic Green's function above is a solution for the dyadic differential equation $\nabla \times \nabla \times \overleftrightarrow{G} - k_o^2 \overleftrightarrow{G} = \overleftrightarrow{I}\delta(r-r')$, $\overleftrightarrow{I} = \hat{x}\hat{x} + \hat{y}\hat{y} + \hat{z}\hat{z}$, instead of the wave equation $(\nabla^2 + k_o^2) \overleftrightarrow{G} = -\overleftrightarrow{I}\delta(r-r')$. It is a complete solution valid both in and out of the source region. Although eq (6) does not have explicity a singular term in the form of $\delta(r-r')$ which normally arises when observing in the source region, this singular term is in fact embedded in it. For our purpose we will retain the modal representation of eq (6) to utilize the symmetry in the dyad.

In computing the fields in a cavity, we resort to numerical computation since $\overleftrightarrow{G}$ is not simple in form. However, since the summation indices of eq (6) extend from 0 to $\infty$, numerical computation of $\overleftrightarrow{G}$ becomes more and more tedious as the observation point approaches the source point. This motivates our search for an alternate representation for the dyad which is more efficient from a computational viewpoint.

In searching for an alternate representation, our approach is to use the Poisson summation transformation to obtain a hybrid ray-mode representation for the dyad. This method of hybrid ray-mode reformulation is not new, being first developed for guided electromagnetic and acoustic fields[5]. For example, in [6,7], the equivalency between mode and ray representations for guided propagation is illustrated by utilizing Poisson summation formulation. Treatment of waveguide fields using hybrid formulation can also be found in [8,9]. Different from the existing work cited above, our treatment is a reformulation for a three-dimensional cavity. We begin our treatment with a description and application of both the infinite and the finite Poisson summation transformations.

## 3. Infinite Poisson Transformation

A one-dimensional Poisson summation formula can be expressed as[10]

$$\sum_{n=-\infty}^{\infty} f(2n\pi) = \frac{1}{2\pi} \sum_{\nu=-\infty}^{\infty} \int_{-\infty}^{\infty} f(\tau)\, e^{i\nu\tau}\, d\tau, \tag{7}$$

provided that

1) f(x) is a continuous and continuously differentiable function of x, and

2) $\sum_{n=-\infty}^{\infty} f(2n\pi+t)$ and $\sum_{n=-\infty}^{\infty} f'(2n\pi+t)$ converge absolutely for all t in the interval $0 \le t \le 2\pi$.

For t=0, the summation reduces to

$$\sum_{n=-\infty}^{\infty} f(2n\pi) = \frac{1}{2\pi} \sum_{\nu=-\infty}^{\infty} \int_{-\infty}^{\infty} f(\tau) e^{i\nu\tau} d\tau. \tag{8}$$

Extending to three-dimensions, we have

$$\sum_{m=-\infty}^{\infty} \sum_{n=-\infty}^{\infty} \sum_{p=-\infty}^{\infty} f(2m\pi,2n\pi,2p\pi) = \tag{9}$$

$$\frac{1}{(2\pi)^3} \sum_{\alpha=-\infty}^{\infty} \sum_{\beta=-\infty}^{\infty} \sum_{\xi=-\infty}^{\infty} \int_{-\infty}^{\infty} \int_{-\infty}^{\infty} \int_{-\infty}^{\infty} f(\tau_1,\tau_2,\tau_3) e^{i(\alpha\tau_1+\beta\tau_2+\xi\tau_3)} d\tau_1 d\tau_2 d\tau_3 .$$

The corresponding f(m,n,p) in the dyadic Green's function expression (eq 3) consists of different combinations of sin() and cos(). For illustratative purposes, we will consider only the case of a scalar Green's function similar in form to the different components embedded in $\overleftrightarrow{G}$. To generalize, a complex wave number $\tilde{k}_o$ will be used to represent the cavity medium.

Consider

$$G(r,r') = \sum_{m=0}^{\infty} \sum_{n=0}^{\infty} \sum_{p=0}^{\infty} \frac{\phi(r)\phi(r')}{\tilde{k}_o^2 - k_\alpha^2}$$

$$=\frac{1}{8}\sum_{m=-\infty}^{\infty}\sum_{n=-\infty}^{\infty}\sum_{p=-\infty}^{\infty}\frac{\phi(r)\phi(r')}{\tilde{k}_o^2 - k_\alpha^2} \tag{10}$$

with

$$\phi(r)= \sin(\frac{m\pi}{a}x)\sin(\frac{n\pi}{b}y)\sin(\frac{p\pi}{c}z). \tag{10a}$$

By letting $k_x=\frac{m\pi}{a}$, $k_y=\frac{n\pi}{b}$, $k_z=\frac{p\pi}{c}$, and expanding $\phi(r)\phi(r')$, we get

$$\phi(r)\phi(r') = \frac{1}{8}[\cos(k_x(x-x'))-\cos(k_x(x+x'))][\cos(k_y(y-y'))-\cos(k_y(y+y'))]\cdot$$
$$[\cos(k_z(z-z'))-\cos(k_z(z+z'))]. \tag{11}$$

By multiplying the bracket terms through, $\phi(r)\phi(r')$ can be decomposed into eight terms, each in the form of $\cos k_xX \cos k_yY \cos k_zZ$, where $X=(x-x')$ or $(x+x')$, $Y=(y-y')$ or $(y+y')$, $Z=(z-z')$ or $(z+z')$. Each of these terms can be further expanded into eight exponential terms in the form of $(\frac{1}{8}e^{i(k_xX+k_yY+k_zZ)})$.

Consider each term separately in the generic form, let

$$f(m,n,p) = \frac{e^{i[k_xX+k_yY+k_zZ]}}{64(\tilde{k}_o^2 - k_\alpha^2)}. \tag{12}$$

Applying the 3-D Poisson summation formula (eq 9) to the summation of $f(m,n,p)$, we get

$$\sum_{m=0}^{\infty}\sum_{n=0}^{\infty}\sum_{p=0}^{\infty} f(2m\pi,2n\pi,2p\pi) = \tag{13}$$

$$\frac{1}{64}\sum_{\alpha=-\infty}^{\infty}\sum_{\beta=-\infty}^{\infty}\sum_{\xi=-\infty}^{\infty}\int_{-\infty}^{\infty}\int_{-\infty}^{\infty}\int_{-\infty}^{\infty}\frac{e^{i(\tau_1\frac{\pi}{a}X+\tau_2\frac{\pi}{b}Y+\tau_3\frac{\pi}{c}Z)+i2\pi(\tau_1\alpha+\tau_2\beta+\tau_3\xi)}}{[\tilde{k}_o^2-((\tau_1\frac{\pi}{a})^2+(\tau_2\frac{\pi}{b})^2+(\tau_3\frac{\pi}{c})^2)]}d\tau_1 d\tau_2 d\tau_3.$$

Using variable changes $k_x = \tau_1 \frac{\pi}{a}$ , $k_y = \tau_2 \frac{\pi}{b}$ , $k_z = \tau_3 \frac{\pi}{c}$ , we can transform the integration to spherical coordinates. The integration with respect to $\theta_k$ and $\phi_k$ can be integrated directly, leaving

$$\sum_{m=0}^{\infty}\sum_{n=0}^{\infty}\sum_{p=0}^{\infty} f(2m\pi,2n\pi,2p\pi) = \left(\frac{abc}{64\pi^3}\right) \sum_{\alpha=-\infty}^{\infty}\sum_{\beta=-\infty}^{\infty}\sum_{\xi=-\infty}^{\infty} \frac{4\pi}{R} \int_0^{\infty} \frac{k \sin(kR)}{(\tilde{k}_o^2 - k^2)} dk, \tag{14}$$

where $k=(k_x^2+k_y^2+k_z^2)^{1/2}$, and $R = R(\alpha,\beta,\xi) = [(X+2a\alpha)^2+(Y+2b\beta)^2+(Z+2c\xi)^2]^{1/2}$. This integral is known exactly as

$$\int_0^{\infty} \frac{k \sin(kR)}{(\tilde{k}_o^2 - k^2)} dk = -\frac{\pi}{2} e^{i\tilde{k}_o R}. \tag{15}$$

Therefore, using the Poisson summation formula, we are able to obtain an alternate expression for the summations of f(m,n,p), i.e.,

$$\sum_{m=0}^{\infty}\sum_{n=0}^{\infty}\sum_{p=0}^{\infty} f(2m\pi,2n\pi,2p\pi) = \frac{abc}{8} \sum_{\alpha=-\infty}^{\infty}\sum_{\beta=-\infty}^{\infty}\sum_{\xi=-\infty}^{\infty} \frac{-e^{i\tilde{k}_o R(\alpha,\beta,\xi)}}{4\pi R(\alpha,\beta,\xi)}. \tag{16}$$

Since f(m,n,p) is only one of the decomposed component of $\phi(r)\phi(r')$, we can perform the similar transformation to every f(m,n,p), and recombine to yield

$$G(r,r') = \sum_{m=0}^{\infty}\sum_{n=0}^{\infty}\sum_{p=0}^{\infty} \frac{\phi(r)\phi(r')}{\tilde{k}_o^2 - k_\alpha^2} = \frac{abc}{8} \sum_{\alpha=-\infty}^{\infty}\sum_{\beta=-\infty}^{\infty}\sum_{\xi=-\infty}^{\infty}\sum_{\ell=1}^{8} (-1)^{\ell} \frac{e^{i\tilde{k}_o R_\ell(\alpha,\beta,\xi)}}{4\pi R_\ell(\alpha,\beta,\xi)}, \tag{17}$$

where

$$R_\ell = [(X_\ell+2a\alpha)^2+(Y_\ell+2b\beta)^2+(Z_\ell+2c\xi)^2]^{1/2}, \tag{17a}$$

$$X_\ell = \begin{cases}(x-x');\ell=1,2,3,4\\(x+x');\ell=5,6,7,8\end{cases}, \quad Y_\ell = \begin{cases}(y-y');\ell=1,2,5,6\\(y+y');\ell=3,4,7,8\end{cases}, \quad Z_\ell = \begin{cases}(z-z');\ell=1,4,6,7\\(z+z');\ell=2,3,5,8.\end{cases}$$

The right side of eq (17) is a summation of the free space Green's function due to sources located at distance $R_\ell$ (see fig. 2). These sources correspond to the image sources resulting from the reflection at the cavity walls. Therefore by the use of the Poisson transformation we are able to obtain a solution which has the physical interpretation of rays emanating from the various image sources. A result similar to eq (17) was obtained by M. Hamid and W. Johnson[11]. Their approach was slightly different in that they started with the right side of eq (17) by invoking the image theorm. The Poisson summation formula was then applied to obtain a modal representation of the Green's function.

## 4. Finite Poisson Transformation

For finite sums over arbitrary intervals, the Poisson summation formula can be expressed as[12]

$$\sum_{\ell=n}^{N} f(\ell) = \sum_{\nu=-\infty}^{\infty} e^{i2\pi\nu(\alpha-1/2)} \int_{n}^{N+1} f(\tau+\alpha-1/2)e^{i2\nu\pi\tau}\, d\tau$$

$$= \sum_{\nu=-\infty}^{\infty} \int_{n+\alpha-1/2}^{N+\alpha+1/2} f(\tau)\, e^{i2\nu\pi\tau} d\tau, \qquad (18)$$

where f(x) is a function of real variable x such that f(x) possesses a Fourier series expansion over any interval in the range $n-\alpha-1/2 < x < N+1-\alpha$. N and n are integers such that $n \le N$, and $\alpha$ is any real number such that $|\alpha| < 1/2$.

For $\alpha=0$, the formula in 3D form can be expressed as

$$\sum_{m=m_o}^{M} \sum_{n=n_o}^{N} \sum_{p=p_o}^{P} f(m,n,p) = \qquad (19)$$

$$\sum_{\alpha=-\infty}^{\infty} \sum_{\beta=-\infty}^{\infty} \sum_{\xi=-\infty}^{\infty} \int_{m_o-1/2}^{M+1/2} \int_{n_o-1/2}^{N+1/2} \int_{p_o-1/2}^{P+1/2} f(\tau_1,\tau_2,\tau_3)e^{i2\pi(\alpha\tau_1+\beta\tau_2+\xi\tau_3)} d\tau_1 d\tau_2 d\tau_3 .$$

Applying eq (19) to the summation of our f(m,n,p) defined in eq (12), we encountered a difficulty in evaluating the triple integration on the right side of eq (19). However, this triple integration can be done in the spherical cooridantes. In transforming to the spherical coordinates, the finite range of summation on the left side of eq (19) can no longer be chosen arbitrarily.

Suppose we select a finite number of sets of (m,n,p) such that the corresponding value of $k_\alpha$ for each mode falls within a spherical shell of width $(k_2-k_1)$, where $k_1 < k_o < k_2$ (see fig. 3). Note that for this selection, the summation limits for each sum on the left side of eq (19), as well as the integration limits on the right side, are no longer independent of one another. As shown in the Appendix, the integration over this special finite range can be approximated by transforming to the spherical coordinates. Referring to the Appendix, the result of this integration is

$$\sum_{S_o}\sum\sum f(m,n,p) \approx \frac{abc}{8} \sum_{\alpha=-\infty}^{\infty} \sum_{\beta=-\infty}^{\infty} \sum_{\xi=-\infty}^{\infty} \frac{1}{8i\pi^2}\, g(\alpha,\beta,\xi); \tag{20}$$

$$g(\alpha,\beta,\xi)= \frac{e^{i\tilde{k}_oR}}{R}[E_1(iR(\tilde{k}_o-k_1))-E_1(iR(\tilde{k}_o-k_2))+E_1(iR(\tilde{k}_o+k_1))-E_1(iR(\tilde{k}_o+k_2))]+$$

$$\frac{e^{-i\tilde{k}_oR}}{R}[E_1(-iR((\tilde{k}_o+k_2))-E_1(-iR(\tilde{k}_o+k_1))+E_1(-iR(\tilde{k}_o-k_1))-E_1(-iR(\tilde{k}_o-k_2))], \tag{21}$$

where R is again defined as $R=[(X+2a\alpha)^2 + (Y+2b\beta)^2 + (Z+2c\xi)^2]^{1/2}$, and $E_1(x)$ is the exponential integral of order 1 defined as $E_1(x) = \int_x^{\infty} \frac{e^{-t}}{t}\,dt$. The spherical shell $S_o$ under the summations represents all the modes (m,n,p) such that $k_1 < k_\alpha < k_2$. Combining eqs (16) and (20), we can write

$$\sum_{m=0}^{\infty}\sum_{n=0}^{\infty}\sum_{p=0}^{\infty} f(m,n,p) \approx \sum_{S_o}\sum\sum f(m,n,p) + \frac{abc}{8} \sum_{\alpha=-\infty}^{\infty} \sum_{\beta=-\infty}^{\infty} \sum_{\xi=-\infty}^{\infty} \tilde{g}(\alpha,\beta,\xi), \tag{22}$$

where

$$\tilde{g}(\alpha,\beta,\xi) = -\frac{e^{i\tilde{k}_oR}}{4\pi R} + \frac{i}{8\pi^2}\, g(\alpha,\beta,\xi).$$

Performing the similar transformation to every decomposed component of $\phi(r)\phi(r')$ and combining with eq (17), the Green's function can now be expressed as

$$\sum_{m=0}^{\infty}\sum_{n=0}^{\infty}\sum_{p=0}^{\infty} \frac{\phi(r)\phi(r')}{\tilde{k}_o^2 - k_\alpha^2} \approx \tag{23}$$

$$\sum\sum\sum_{S_o} \frac{\phi(r)\phi(r')}{\tilde{k}_o^2 - k_\alpha^2} + \frac{abc}{8}\sum_{\alpha=-\infty}^{\infty}\sum_{\beta=-\infty}^{\infty}\sum_{\xi=-\infty}^{\infty}\sum_{\ell=1}^{8}(-1)^\ell \left\{\frac{e^{i\tilde{k}_o R_\ell}}{4\pi R_\ell} + \frac{1}{8\pi^2 i}\, g(\alpha,\beta,\xi;R_\ell)\right\},$$

where $R_\ell$ is defined in eq (17a), and $g(\alpha,\beta,\xi;R_\ell)$ is defined in eq (21) with R replaced by $R_\ell$. For ease of identification, we refer to the finite range sum of eq (23) as the mode sum, the second sum involving $(\alpha,\beta,\xi)$ as the ray sum, and the sum on the left side of eq (23) as the triple sum.

For the special case of real instead of complex wave number $k_o$, the expression for $g(\alpha,\beta,\xi;R)$ becomes

$$g(\alpha,\beta,\xi) = \frac{2i\cos(k_o R)}{R}[Si(R(k_o-k_2))-Si(R(k_o-k_1))+Si(R(k_o+k_1))-Si(R(k_o+k_2))]$$

$$+ \frac{2i\sin(k_o R)}{R}[Ci(R(k_o-k_1))-Ci(R(k_o-k_2))+Ci(R(k_o+k_2))-Ci(R(k_o+k_1))], \tag{24}$$

where Si and Ci are the sine and cosine integrals defined as $Si(x)=\int_0^x \frac{\sin t}{t}dt$, $Ci(x)=-\int_x^\infty \frac{\cos t}{t}dt$. If we choose $S_o$ to be symmetrical about $k_o$ so that $k_1=k_o-\gamma$, and $k_2=k_o+\gamma$, where $2\gamma$ is the summation shell width, eq (23) can be simplified to

$$G(r,r') \approx \sum\sum\sum_{S_o} \frac{\phi(r)\phi(r')}{k_o^2 - k_\alpha^2} + \tag{25}$$

$$\frac{abc}{8}\sum_{\alpha=-\infty}^{\infty}\sum_{\beta=-\infty}^{\infty}\sum_{\xi=-\infty}^{\infty}\sum_{\ell=1}^{8}(-1)^\ell \left\{\frac{\cos(k_o R_\ell)}{4\pi R_\ell}\left(1-\frac{2}{\pi}\,Si(\gamma R_\ell)\right)-\Delta_\ell\right\},$$

where

$$\Delta_\ell = \frac{\cos(k_o R_\ell)}{4\pi^2 R_\ell} [Si(R_\ell(2k_o+\gamma)) - Si(R_\ell(2k_o-\gamma))] - \frac{\sin(k_o R_\ell)}{4\pi^2 R_\ell} [Ci(R_\ell(2k_o+\gamma)) - Ci(R_\ell(2k_o-\gamma))]. \qquad (25a)$$

For $\gamma \ll k_o$, $\Delta_\ell$ contributes only a negligible amount. When $k_o R_\ell$ is small, the ray sum is dominated by $\frac{\cos(k_o R_\ell)}{4\pi\ R_\ell}$, and when $\gamma R_\ell$ is large, the image terms are oscillatory and are weighted by $(1/R_\ell^2 \gamma)$.

A balancing effect exists between the mode sum and the ray sum. When we increase $\gamma$, i.e. increase the bandwidth for the mode sum, the number of modes that fall within the band will be increased. Therefore the contribution from the mode sum will be increased at the same time the quantity $(1-\frac{2}{\pi}Si(R_\ell \gamma))$ decreases, thus reducing the contribution from the ray sum.

When the dimensions of the cavity are large and the observation point is close to the source point (but not close to the wall), the ray sum will be dominated by the self term, $\frac{\cos(k_o R_o)}{4\pi R_o}$, $R_o = [(x-x')^2+(y-y')^2+(z-z')^2]^{1/2}$. For a very large cavity, $\gamma R_\ell$ can be large for all image terms if $\gamma$ is not too small, so the contribution from all the images is of the order $(\frac{1}{R_\ell^2 \gamma})$ smaller. Therefore for a source located not near the wall, we can approximate eq (25) further to yield

$$\sum_{m=0}^{\infty}\sum_{n=0}^{\infty}\sum_{p=0}^{\infty}\frac{\phi(r)\phi(r')}{k_o^2 - k_\alpha^2} \approx \sum\sum\sum_{S_o}\frac{\phi(r)\phi(r')}{k_o^2 - k_\alpha^2} - \frac{abc}{8}\left\{\frac{\cos(k_oR_o)}{4\pi R_o}\left(1-\frac{2}{\pi}Si(\gamma R_o)\right) - \Delta_o\right\}, \tag{26}$$

where the correction,

$$\Delta_o = \frac{\cos(k_oR_o)}{4\pi^2 R_o}[Si(R_o(2k_o+\gamma))-Si(R_o(2k_o-\gamma))] - \frac{\sin(k_oR_o)}{4\pi^2 R_o}[Ci(R_o(2k_o+\gamma))-Ci(R_o(2k_o-\gamma))] \tag{26a}$$

contributes a negligible amount. Numerical data showing the closeness of this approximation will be presented in the next section, along with the criterion for choosing a minimum $\gamma$.

Although eq (26) is only an approximation to the exact expression, addition of a few or more images will not necessarily improve the approximation. This is so because while the higher order images are decaying at the rate of $1/R^2$, the number of images is increasing at the rate proportioned to $R^2$. Therefore the summation of the remaining terms is likely to be a slow but bounded oscillatory term of order O(1). This contribution is small only because the mode sum usually has a large amplitude, i.e. $(k_o^2 - k_\alpha^2)^{-1} >> 1$ near resonance. As will be seen in the numerical examples in the next section, retaining only those images with $k_oR_\ell << 1$ is sufficient to yield satisfactory agreement with the numerically "exact" answer.

For the case when the cavity is lossy, $\tilde{k}_o$ is complex, i.e. $\tilde{k}_o=k_o+i\gamma_o$, where $\gamma_o$ is usually associated with the loss in the cavity. Expressions for

$g(\alpha,\beta,\xi;R_{\ell})$ for $|\gamma_o R| >> 1$ and $|\tilde{k}_o R| << 1$ are given respectively in the Appendix.

## 5. Numerical Examples

To simplify computations, we assume $k_o$ is real and the cavity is cubic. The frequency of operation is fixed at 1 GHz. Two cases will be considered. In case 1 we fix the source point near the center of the cavity and vary the observation distance. In case 2 we vary the source point along a vertical axis and show that when the source point is close to the wall, the first image must be included in eq (26) to achieve a good approximation.

In evaluating the triple sum, $\sum_{m=0}^{\infty}\sum_{n=0}^{\infty}\sum_{p=0}^{\infty} \dfrac{\phi(r)\phi(r')}{k_o^2 - k_\alpha^2}$ is first reduced to a double sum using the known summation result[13],

$$\sum_{n=0}^{\infty} \frac{\cos(nx)}{n^2 - \xi^2} = -\frac{1}{2\xi^2} - \frac{\pi\cos(x-\pi)\xi}{2\xi\ \sin\pi\xi} \quad ; \quad 0 \le x \le 2\pi. \qquad (27)$$

The variable $\xi$ in eq (27) becomes imaginary when $(k_x^2 + k_y^2) > k_o^2$. For imaginary $\xi$, the summation function becomes exponential functions that decay rapidly as either $k_x$ or $k_y$ approaches infinity. Thus the resulting sums can in fact be truncated. At the expense of long computation time, the reduced summations are summed with indices extending from 0 to a large number M. To minimize error, care is taken in the determination of M to ensure that the remaining sum from M to $\infty$ is neglibible compared to the sum from 0 to M. Typically 90000 terms are needed to yield an error of less than 1 percent for $k_o R_o \ge 0.15\pi$.

The length of the cubic cavity is arbitrarily chosen to be $15.23\lambda$. Unless indicated otherwise, the ray sum consists of only the self term (eq 26).

## 5.1 Case I: Centered source point

With the source point at the center, figure 4 shows the variations of the mode sum, the hybrid sum, and the triple sum with $k_oR_o$ varying from $1.0\pi$ to $10\pi$, and figure 5 has $k_oR_o$ varying from $0.2\pi$ to $1.0\pi$. $R_o$ is the distance between the source and the observation point. $\gamma$ is chosen to be $(0.01)k_o$, which corresponds to 831 modes for the size of cavity chosen. Within the range of small $k_oR_o$, especially at $k_oR_o < 1.0\pi$, the self term plays an important role. With just the self term included, the hybrid sum provides a very good approximation to the triple modal sum.

As $k_oR_o$ increases, the self term loses its dominant effect. At large $k_oR_o$, i.e. $k_oR_o \geq 5\pi$, every term in the ray sum, including the self term, becomes very small. Therefore the contribution on the right side of eq (26) comes directly from the finite mode sum as is evident in figure 4.

At the intermediate range of $k_oR_o$ ($0.4\pi \leq k_oR_o \leq 5\pi$), the contribution from the self term is losing its dominant effect, but it is not quite small enough to be totally negligible. To further close the gap between the hybrid sum representation and the triple sum, one either has to sum all of the image terms or increase the bandwidth to increase the contribution from the mode sum. Figure 6 shows the effect of increasing bandwidth for $k_oR_o$ in the range $0.9\pi \leq k_oR_o \leq 1.0\pi$. As can be seen, the process of increasing bandwidth produces a very slow converging effect; at the same time the computation time for the mode sum increases proportionally to the number of modes involved. Since neither summing more images, as discussed earlier, nor increasing the bandwidth provides a feasible way to close the gap, we may have to accept the slight deviation from the exact value in exchange for long computation time for $k_oR_o$ in this intermediate range.

## 5.2 Case II: Off-centered source point

Figures 7 and 8 show the variations of the mode sum, the hybrid sum, and the triple sum as the source point is varied. The self term $k_oR_o$ remains fixed at $0.2\pi$ throughout, while $k_oR_1$ is varied from $0.3\pi$ to $10\pi$ (see fig. 9). With the first image term included, eq (26) becomes

$$\sum_{m=0}^{\infty}\sum_{n=0}^{\infty}\sum_{p=0}^{\infty} \frac{\phi(r)\phi(r')}{k_o^2 - k_\alpha^2} \approx \sum\sum\sum_{S_o} \frac{\phi(r)\phi(r')}{k_o^2 - k_\alpha^2} - \tag{28}$$

$$\frac{abc}{8}\sum_{\ell=0,1} (-1)^\ell \left\{\frac{\cos(k_oR_\ell)}{4\pi R_\ell}\left(1-\frac{2}{\pi}Si(R_\ell\gamma)\right) - \Delta_\ell\right\},$$

$$\Delta_\ell = \frac{\cos(k_oR_\ell)}{4\pi^2 R_\ell}[Si(R_\ell(2k_o+\gamma))] - \frac{\sin(k_oR_\ell)}{4\pi^2 R_\ell}[Ci(R_\ell(2k_o+\gamma))-Ci(R_\ell(2k_o-\gamma))]$$

$$R_o = [(x-x')^2 + (y-y')^2 + (z-z')^2]^{1/2} \tag{28a}$$

$$R_1 = [(x-x')^2 + (y-y')^2 + (z-(2c-z'))^2]^{1/2}.$$

When the source is close to the wall, i.e. when $k_oR_1$ is small, the addition of the first image term becomes essential. Figure 8 shows that, without the addition of the first image term, the self term alone is not enough for the equality to hold in eq (26). As the source is moved away from the wall, i.e. $k_oR_1$ is increased, figure 7 shows that the contribution from the first image in eq (28) becomes small (almost negligible at $k_oR_1 \geq 6\pi$). With large $k_oR_1$, we revert back to case I where the self term is dominant.

In the above computations, we have chosen $\gamma$ to be $(0.01)k_o$. Increasing $\gamma$ increases the number of modes in the band, which may increase the computation time if the number of modes in the mode sum is large. However, while decreasing the shell bandwidth may decrease the computation time, it may also introduce an approximation error which may cause eq (20) to become invalid if $\gamma$ is too small. To show this we must go back to the derivation of eq (20) in the Appendix.

In figure A-2 we show the approximation made for the shaded grid area with the spherical shell. The shaded area represents the range of integration for the function $F(\alpha,\beta,\xi)$. Although we can arbitrarily choose the number of grids to match the shell, each grid has a minimum width since the minimum increment of (m,n,p) must be 1, i.e. the minimum summation interval must be from $(m_o,n_o,p_o)$ to $(m_o+1,n_o+1,p_o+1)$. The minimum grid width is therefore $\pi/a$ where a corresponds to the smallest dimension of the cavity size. For our choice of $a=15.23\lambda$ and $\gamma=0.01k_o$, we have a shell width to minimum grid width ratio of approximately 0.6, i.e.

$$\text{width ratio} = \frac{2\gamma}{\pi/a} \approx 0.6. \tag{29}$$

This width ratio of 0.6 was determined numerically to be adequate in approximating the grid area with the shell. We need not go to a full width ratio of 1.0 because the integrand $F(\alpha,\beta,\xi)$ has the greatest value at k near $k_o$, and it decays down as k is moved away from $k_o$. As the width ratio is decreased below 0.6, the approximation illustrated in figure A-2 becomes poor, and eq (20) (and thus eq 26) becomes a poor approximation.

To illustrate the effect of different shell widths, figure 10 shows the variation of the hybrid sum for $0.3\pi \le k_oR_o \le 0.4\pi$ as the width ratio is decreased below 0.6. With a very small width ratio, the deviation between the hybrid sum and the triple sum is indeed not acceptable. A width ratio of 0.6 represents a conservative choice in that a smaller width ratio of 0.4 or 0.5 may work just as well as 0.6. For width ratios greater than 0.6, we get into the region of slow convergence and increasing computation time. This tradeoff does not seem to be worthwhile for choosing a width ratio greater than 0.6.

## 6. Conclusion

In this report we have shown that the Green's function for a rectangular cavity in the modal representation form can be transformed into a hybrid representation consisting of a finite mode sum and a sum over all the images. This hybrid sum was effective because it allowed for the disposal of all the distance image terms without suffering an unacceptable loss of numerical accuracy. When the observation point was very close to the source point, and when the source was not close the wall, we have shown numerically that retaining just the self term in the ray sum was sufficient to yield a good approximation of the triple modal sum. When the source was close to the wall the first image term became important. The hybrid representation developed in this report is valid for either real or complex $k_o$. Except for the requirement that the bandwidth chosen for the mode sum is not too small (width ratio above 0.6), the hybrid representation is in general a good approximation of the modal representation, and it possesses unique properties that allow for feasible numerical evaluation.

With this alternate representation, the effect of a scatterer in a large rectangular cavity can now be examined numerically. The scattered field can be computed once the induced current on the scatterer is known. As illustrated in [14], this hybrid Green's function is most useful in the numerical computations of the induced current $\vec{J}$ and the corresponding scattered field for a simple-structured scatterer in a rectangular cavity.

References

[1] Corona, P.; Latmiral, G.; Paolini, E.; and Piccioli, L. Use of a reverberating enclosure for measurements of radiated power in the microwave range. IEEE Trans. on EMC, EMC-22: 54-59; 1976.

[2] Liu, B. H.; Chang, D. C.; and Ma, M. T. Eigenmodes and the composite quality factor of a reveberating chamber. Nat. Bur. Stand. (U.S.) NBS Tech Note 1066; 1983 August.

[3] Ghose, R. N. Microwave circuit theory and analysis. New York, NY: McGraw Hill; 1963.

[4] Harrington, R. F. Time-harmonic electromagnetic fields. New York, NY: McGraw Hill; 1961.

[5] Felsen, L. B. Hybrid formulation of wave propagation and scattering. Dordrecht, The Netherlands: Martinus Nijhoff; 1984. 3-21.

[6] Gao, T. F.; Shang, E. C. The transformation between the mode representation and the generalized ray representation of a sound field. J. Sound Vib. Vol. 80: 105-115; 1982.

[7] Kamel, A.; Felsen, L. B. On the ray equivalent of a group of modes. J. Acoust. Soc. Am., Vol. 71: 1447-1452; 1982.

[8] Felsen, L. B.; Kamel, A. Hybrid ray-mode formulation of parallel waveguide Green's functions. IEEE Trans. AP, AP-29: 637-649; 1981

[9] Ishihara, T.; Felsen, L. B.; Green, A. High frequency fields excited by a line source on a perfectly conducting concave cylindrical surface. IEEE Trans. AP, AP-26: 757-767; 1978.

[10] Courant, R.; Hilbert, D. Methods of mathematical physics. Vol. 1 New York, NY: Interscience; 1962.

[11] Hamid, M. A. K.; and Johnson, W. A. Ray-optical solution for the dyadic Green's function in a rectangular cavity. Electronics Letters, Vol. 6, No. 10: 317-319; 1970 May.

[12] Crowley, B. J. B. Some generalisation of the Poisson summation formula. J. Phys. A: Math. Gen., Vol. 12, No. 11: 1951-1955; 1979.

[13] Collin, R. E. Field theory of guided waves. New York, NY: McGraw Hill; 1960.

[14] Wu, D. I. On the effect of a rotating scatterer in an over-moded rectangular cavity. Ph.D. dissertation, Univ. of Colorado, Boulder, CO. May 1987.

APPENDIX

Summing Over Finite Intervals

Consider a finite range triple summation defined as

$$Q = \sum_{m=m_o}^{M} \sum_{n=n_o}^{N} \sum_{p=p_o}^{P} f(m,n,p) = \sum_{m=m_o}^{M} \sum_{n=n_o}^{N} \sum_{p=p_o}^{P} \frac{e^{i(\frac{m\pi}{a} X+\frac{n\pi}{b} Y+\frac{p\pi}{c} Z)}}{(\tilde{k}_o^2 - k_\alpha^2)} . \tag{A1}$$

Applying the finite Poisson formula (eq 19), and letting $k_x=\tau_1\frac{\pi}{a}$, $k_y=\tau_2\frac{\pi}{b}$, $k_z=\tau_3\frac{\pi}{c}$, eq (A1) becomes

$$Q = (\frac{abc}{64\pi^3}) \sum_{\alpha=-\infty}^{\infty} \sum_{\beta=-\infty}^{\infty} \sum_{\xi=-\infty}^{\infty} \int_{x_1}^{x_2} \int_{y_1}^{y_2} \int_{z_1}^{z_2} F(\alpha,\beta,\xi)\, dk_x dk_y dk_z , \tag{A2}$$

where

$$\begin{aligned} x_1 &= (m_o-1/2)\frac{\pi}{a} , \quad x_2 = (M+1/2)\frac{\pi}{a} , \\ y_1 &= (n_o-1/2)\frac{\pi}{b} , \quad y_2 = (N+1/2)\frac{\pi}{b} , \\ z_1 &= (p_o-1/2)\frac{\pi}{c} , \quad z_3 = (P+1/2)\frac{\pi}{c} , \end{aligned} \tag{A3}$$

and

$$F(\alpha,\beta,\xi) = \frac{e^{i[k_x(X+2a\alpha)+k_y(Y+2b\beta)+k_z(Z+2c\xi)]}}{\tilde{k}_o^2 - (k_x^2 + k_y^2 + k_z^2 )} . \tag{A4}$$

The summation intervals on the left side transform directly into integration limits on the right side with a small amount of shifting given by ±1/2. A typical range of integration corresponds to the shaded area in figure A-1 with each grid on the figure corresponding to a different set of summation interval $(m_o, n_o, p_o)$ to $(M_o, N_o, P_o)$.

Suppose we now arbitrarily select a finite set of grids (or summation intervals) such that they are clustered around $k_o$ as shown in figure A-2. Then

$$\left[\sum_{m_o}^{M_o}\sum_{n_o}^{N_o}\sum_{p_o}^{P_o} + \ldots + \sum_{m_\ell}^{M_\ell}\sum_{n_\ell}^{N_\ell}\sum_{p_\ell}^{P_\ell}\right] f(m,n,p) = \tag{A5}$$

$$\left(\frac{abc}{64\pi^3}\right)\sum_{\alpha=-\infty}^{\infty}\sum_{\beta=-\infty}^{\infty}\sum_{\xi=-\infty}^{\infty}\left[\int\int\int_{\text{grid1}} + \ldots + \int\int\int_{\text{grid}\ell}\right] F(\alpha,\beta,\xi)dk_x dk_y dk_z .$$

We now make the approximation,

$$\left[\int\int\int_{\text{grid1}} + \ldots + \int\int\int_{\text{grid}\ell}\right] F(\alpha,\beta,\xi)dk_x dk_y dk_z \approx \int\int\int_{V_o} F(\alpha,\beta,\xi)dk_x dk_y dk_z , \tag{A6}$$

where $V_o$ is the volume of the spherical shell bounded by $k_1$ and $k_2$, and

$$\left[\sum_{m_o}^{M_o}\sum_{n_o}^{N_o}\sum_{p_o}^{P_o} + \ldots + \sum_{m_\ell}^{M_\ell}\sum_{n_\ell}^{N_\ell}\sum_{p_\ell}^{P_\ell}\right] f(m,n,p) \approx \sum\sum\sum_{S_o} f(m,n,p), \tag{A7}$$

where the $S_o$ notation represents all the modes, $(m,n,p)$, that fall within the spherical shell. Combining eqs (A6) and (A7) above, we get

$$\sum\sum\sum_{S_o} f(m,n,p) \approx \tag{A8}$$

$$\left(\frac{abc}{64\pi^3}\right)\sum_{\alpha=-\infty}^{\infty}\sum_{\beta=-\infty}^{\infty}\sum_{\xi=-\infty}^{\infty}\int\int\int_{V_o} \frac{e^{i[k_x(X+2a\alpha)+k_y(Y+2b\beta)+k_z(Z+2c\xi)]}}{\tilde{k}_o^2 - (k_x^2 + k_y^2 + k_z^2)} dk_x dk_y dk_z .$$

Transforming to spherical coordinates, and letting

$$k^2 = k_x^2 + k_y^2 + k_z^2,\quad dk_x dk_y dk_z = k^2 \sin\theta_k dk d\theta_k d\phi_k,$$

$$k_x = k\sin\theta_k\cos\phi_k,\quad k_y = k\sin\theta_k\sin\phi_k,\quad k_z = k\cos\theta_k, \tag{A9}$$

$$\rho = [(X+2a\alpha)^2 + (Y+2b\beta)^2]^{1/2},\quad \phi_{\alpha\beta} = \tan^{-1}\left(\frac{Y+2b\beta}{X+2a\alpha}\right),\quad R = [\rho^2 + (Z+2c\xi)^2]^{1/2},$$

we obtain

$$\sum_{S_o}\sum\sum f(m,n,p)$$

$$\approx\left(\frac{abc}{64\pi^3}\right)\int_{k_1}^{k_2}\frac{k^2 dk}{\tilde{k}_o^2 - k^2}\int_0^{\pi}\sin\theta_k d\theta_k\int_0^{2\pi} e^{i\rho k\sin\theta_k\cos(\phi_k+\phi_{\alpha\beta})+ik\cos\theta_k(Z+2c\xi)}d\phi_k$$

$$=\left(\frac{abc}{64\pi^3}\right)4\pi\int_{k_1}^{k_2}\frac{k\sin(kR)}{R(\tilde{k}_o^2 - k^2)}dk$$

$$=\left(\frac{abc}{64i\pi^2}\right)g(\alpha,\beta,\xi) \tag{A10}$$

where

$$g(\alpha,\beta,\xi) = \frac{e^{i\tilde{k}_o R}}{R}[E_1(iR(\tilde{k}_o - k_2)) - E_1(iR(\tilde{k}_o - k_1)) + E_1(iR(\tilde{k}_o + k_1)) - E_1(iR(\tilde{k}_o + k_2))] +$$

$$\frac{e^{-i\tilde{k}_o R}}{R}[E_1(-iR(\tilde{k}_o + k_2)) - E_1(-iR(\tilde{k}_o + k_1)) + E_1(-iR(\tilde{k}_o - k_1)) - E_1(-iR(\tilde{k}_o - k_2))], \tag{A11}$$

or equivalently

$$g(\alpha,\beta,\xi) = \frac{2i\cos(\tilde{k}_o R)}{R}[\mathrm{Si}(R(\tilde{k}_o - k_2)) - \mathrm{Si}(R(\tilde{k}_o - k_1)) + \mathrm{Si}(R(\tilde{k}_o + k_1)) - \mathrm{Si}(R(\tilde{k}_o + k_2))] +$$

$$\frac{2i\sin(\tilde{k}_o R)}{R}[\mathrm{Ci}(R(\tilde{k}_o - k_1)) - \mathrm{Ci}(R(\tilde{k}_o - k_2)) - \mathrm{Ci}(R(\tilde{k}_o + k_1)) + \mathrm{Ci}(R(\tilde{k}_o + k_2))]. \tag{A12}$$

$E_1$ is the exponential integral function defined as $E_1(z)=\int_z^\infty \frac{e^{-t}}{t}dt$. Si and Ci are the sine and cosine integrals defined as $Si(z) = \int_0^z \frac{\sin t}{t}dt$, and $Ci(z) = -\int_z^\infty \frac{\cos t}{t}dt$.

Therefore using Poisson summaton formula, we can write

$$\sum_{S_o}\sum\sum f(m,n,p) \approx \left(\frac{abc}{64i\pi^2}\right) \sum_{\alpha=-\infty}^{\infty} \sum_{\beta=-\infty}^{\infty} \sum_{\xi=-\infty}^{\infty} g(\alpha,\beta,\xi). \tag{A13}$$

If we let $\tilde{k}_o=k_o+i\gamma_o$, $k_1=k_o-\gamma_1$, $k_2=k_o+\gamma_1$, then for small argument, i.e. $|k_oR| << 1$, $E_1(z)\approx-\gamma-\ln(z)$ where $\gamma$ is the Euler constant, $g(\alpha,\beta,\xi)$ becomes

$$g(\alpha,\beta,\xi) \approx \frac{i\sin(\tilde{k}_oR)}{R}\left[-2i\pi+4\tan^{-1}(\gamma_o/\gamma_1)+2\ln\left(\frac{2k_o+\gamma_o(i+\gamma_1/\gamma_o)}{2k_o+\gamma_o(i-\gamma_1/\gamma_o)}\right)\right]. \tag{A14}$$

For large argument, i.e. $|\gamma_oR| >> 1$, $Si(z)\approx\frac{\pi}{2} - \frac{\cos z}{z}$, $Ci(z)\approx\frac{\sin z}{z}$, and using expression A12, $g(\alpha,\beta,\xi)$ becomes

$$\frac{g(\alpha,\beta,\xi)}{8i\pi^2} \approx - \frac{e^{i\tilde{k}_oR}}{4\pi R} + \tag{A15}$$

$$\frac{1}{4\pi^2R^2}\left[\frac{\cos(R(k_o+\gamma_1))}{\gamma_1 - i\gamma_o} + \frac{\cos(R(k_o-k_1))}{\gamma_1 + i\gamma_o} - \frac{\cos(R(\gamma_1-k_o))}{2k_o+ i\gamma_o+ \gamma_1} + \frac{\cos(R(\gamma_1+k_o))}{2k_o+ i\gamma_o- \gamma_1}\right] + O\left(\frac{1}{R^3}\right).$$

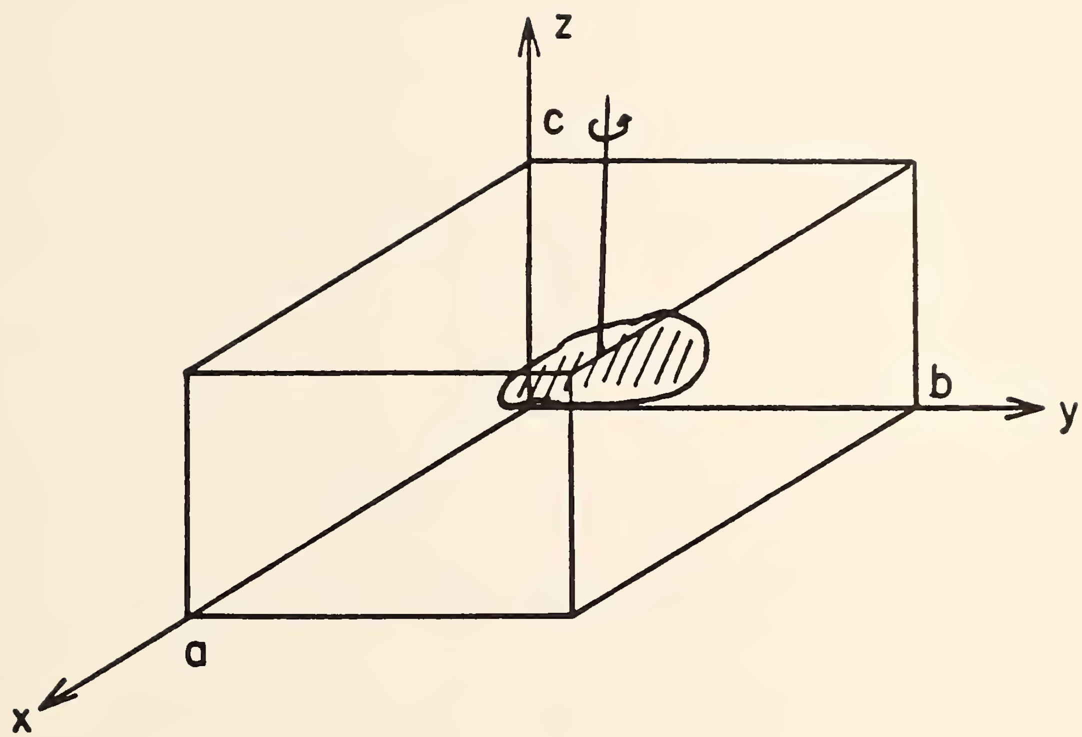


Figure 1: A rectangular cavity with a perfectly conducting scatterer.

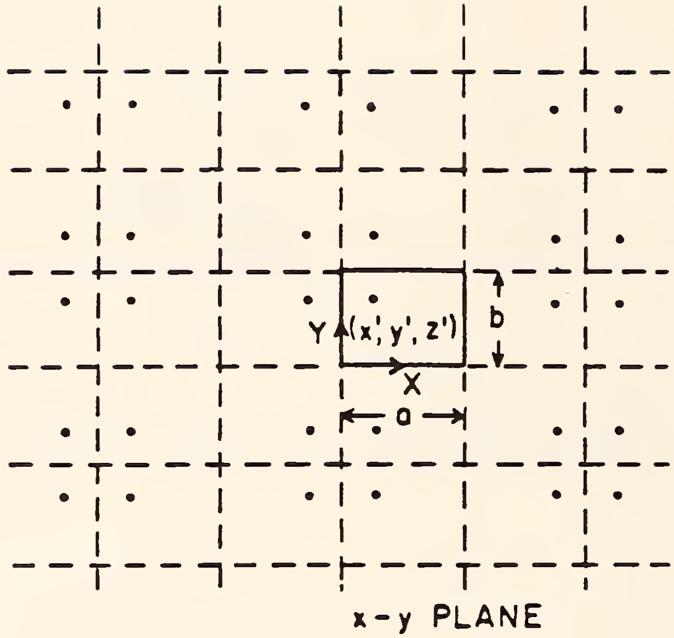


Figure 2: Equivalent image sources in free space.

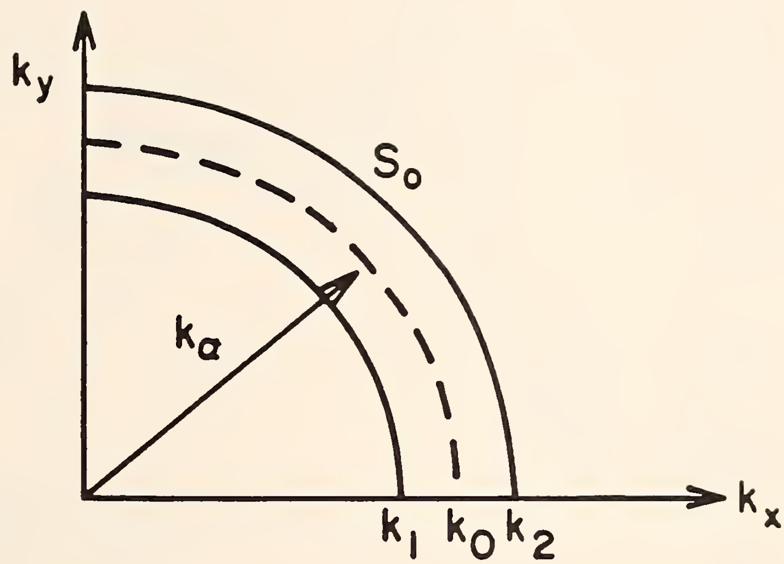


Figure 3: A summation shell.

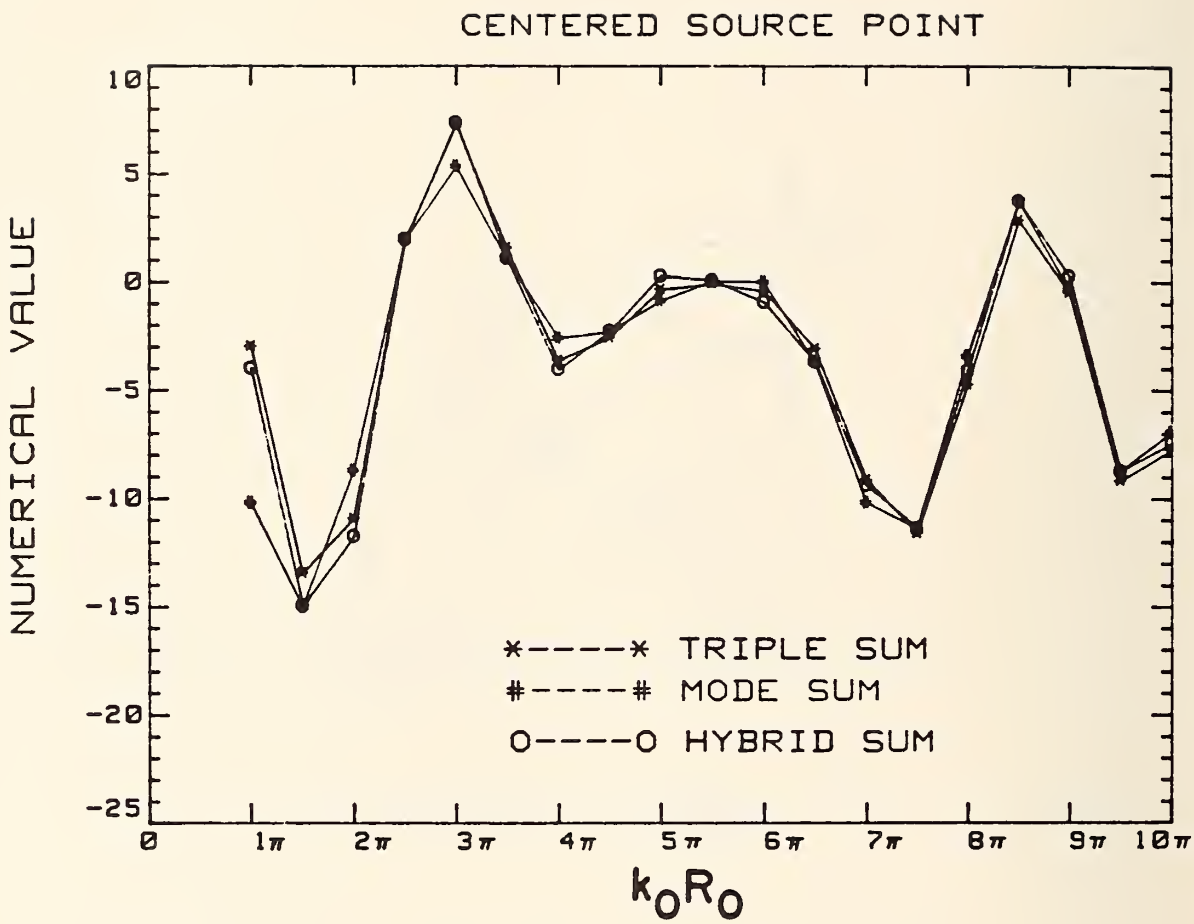


Figure 4: Comparison of the mode sum and the hybrid sum with $G(r,r')$ for centered source point with $1.0\pi < k_o R_o < 10\pi$.

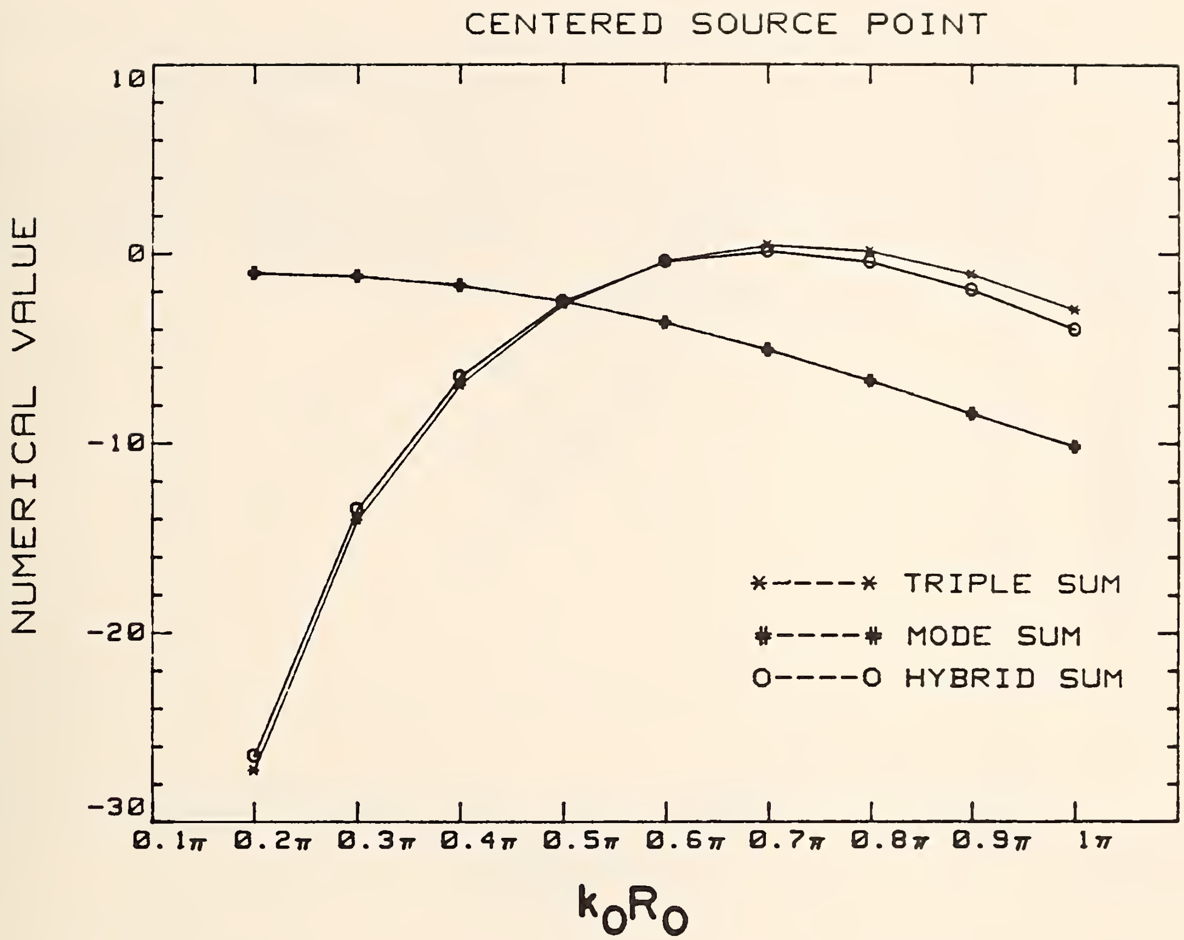


Figure 5: Comparison of the mode sum and the hybrid sum with $G(r,r')$ for centered source point with $0.2\pi < k_oR_o < 1.0\pi$.

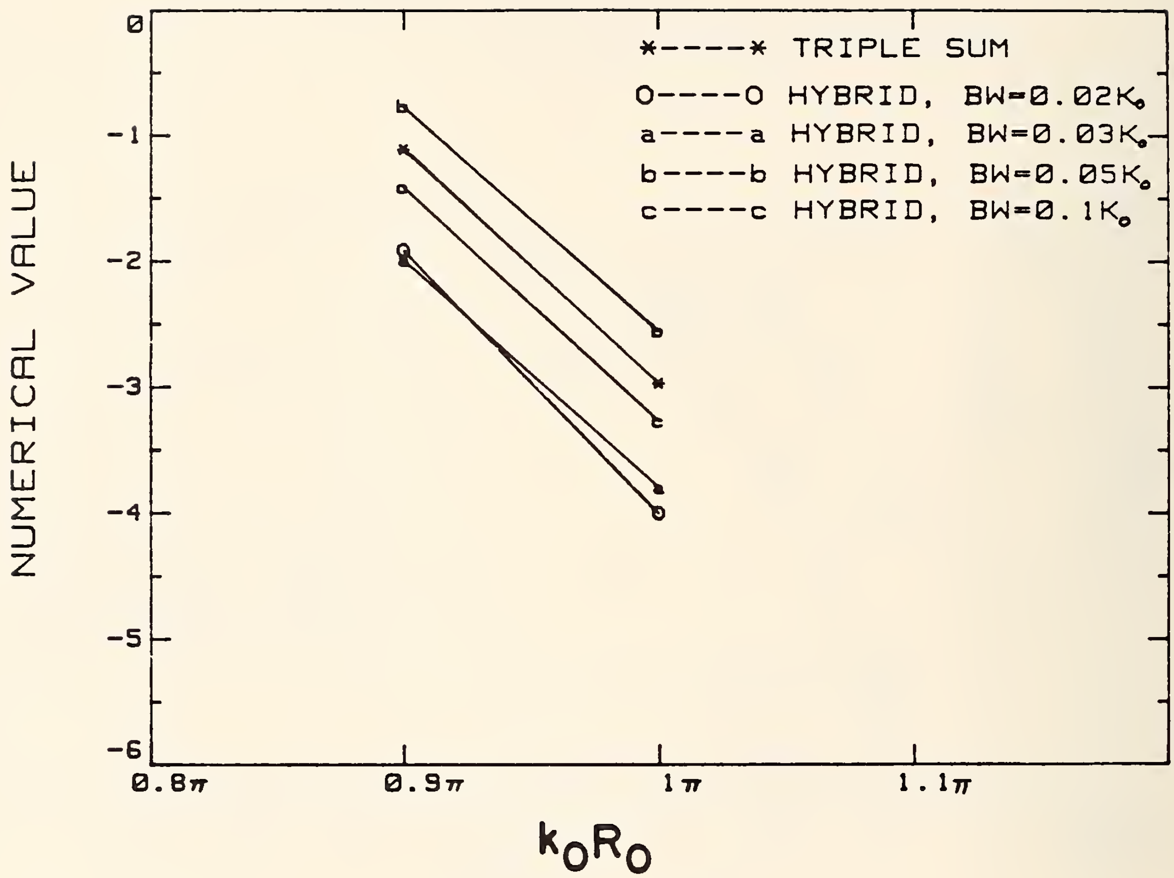


Figure 6: Comparison of the hybrid sum with G(r,r′) for different summation bandwidths.

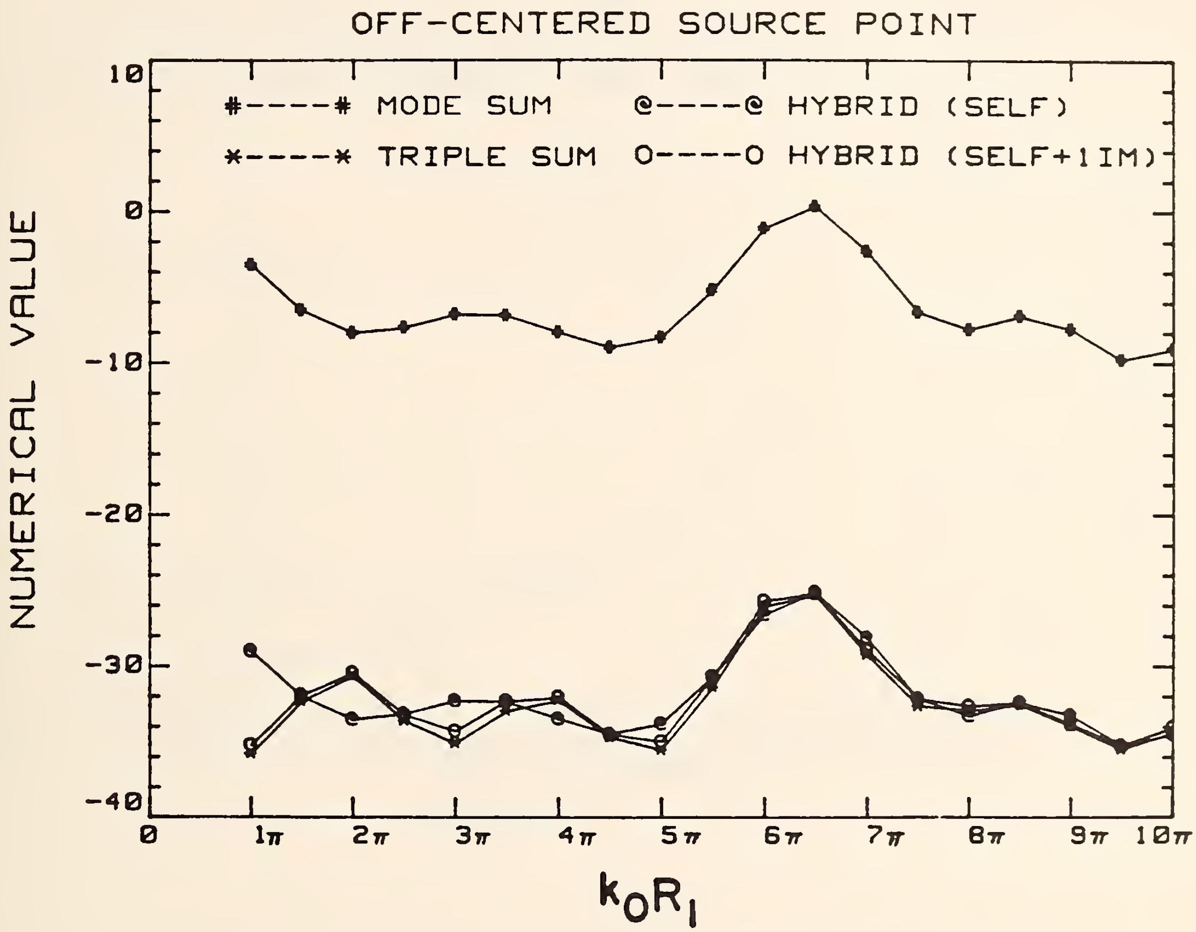


Figure 7: Comparison of the mode sum and the hybrid sum with $G(r,r')$ for off-centered source point with $1.0\pi \le k_oR_1 \le 10\pi$.

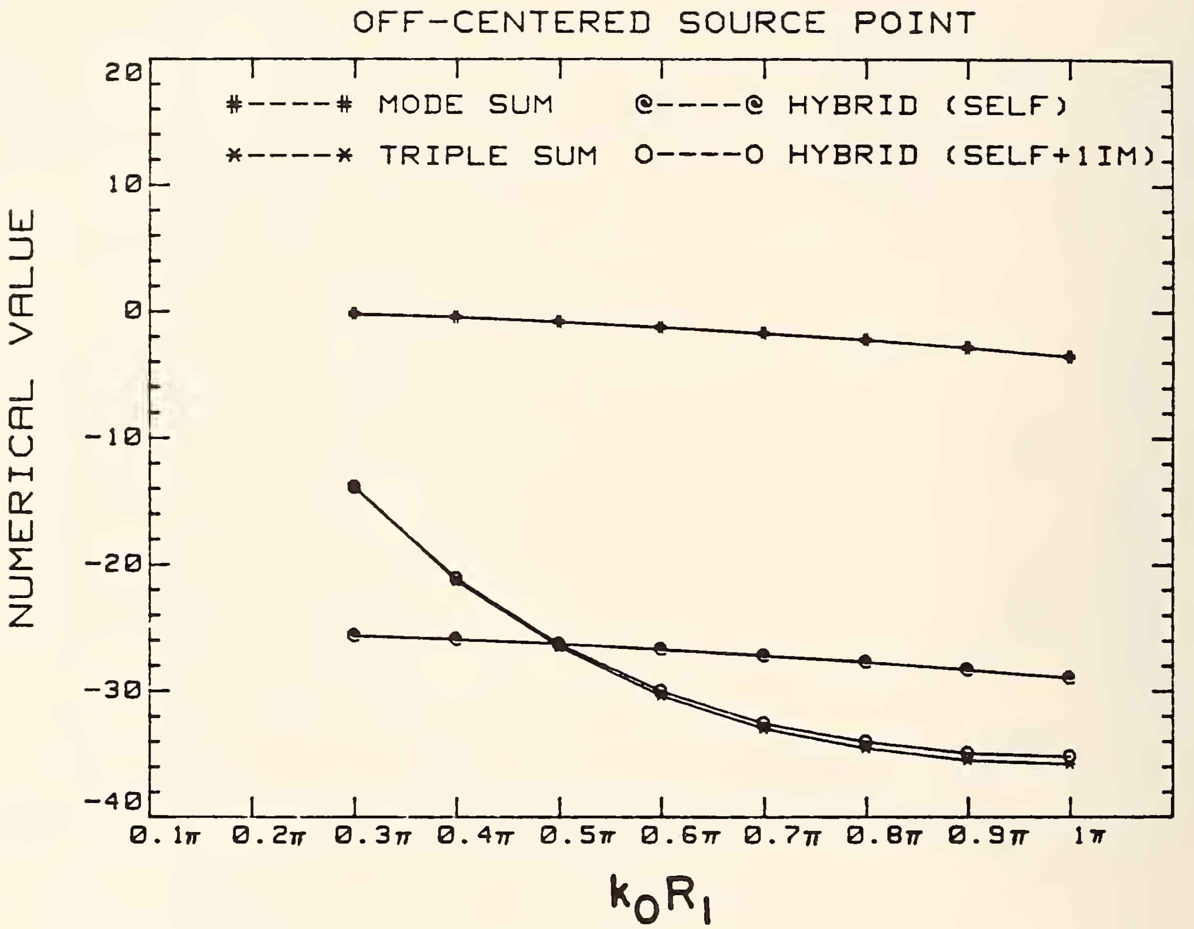


Figure 8: Comparison of the mode sum and the hybrid sum with $G(r,r')$ for off-centered source point with $0.3\pi \le k_oR_1 \le 1.0\pi$.

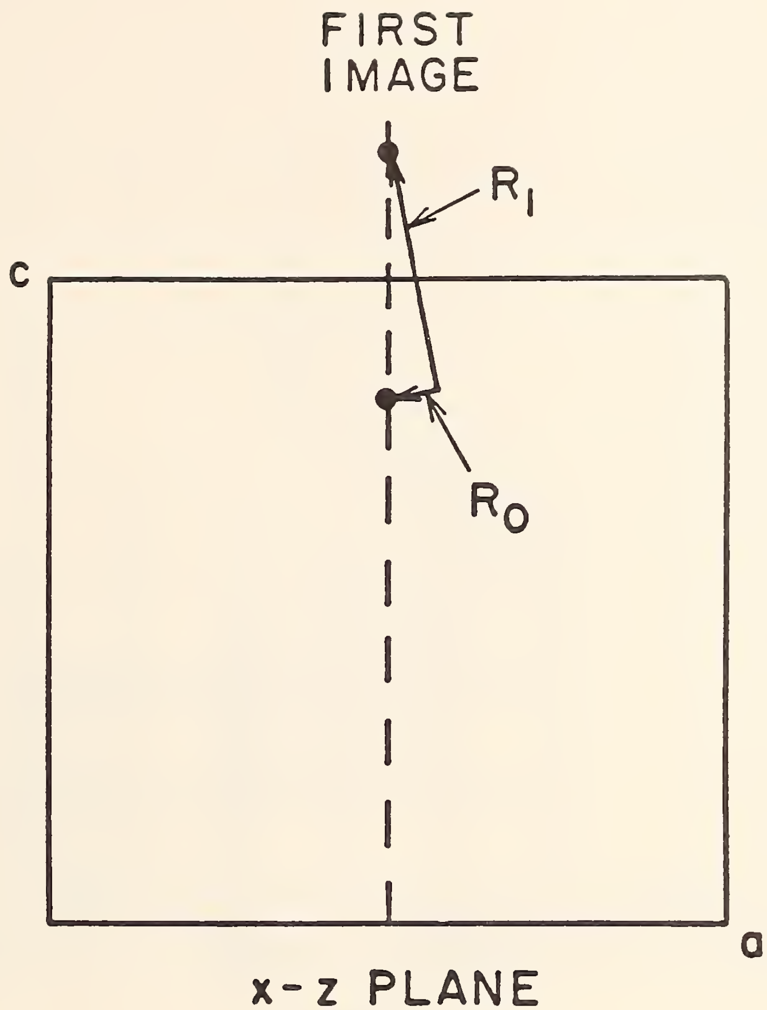


Figure 9: A cross-sectional view of the first image distance $R_1$ and the distance $R_o$ between the source and the obersvation point.

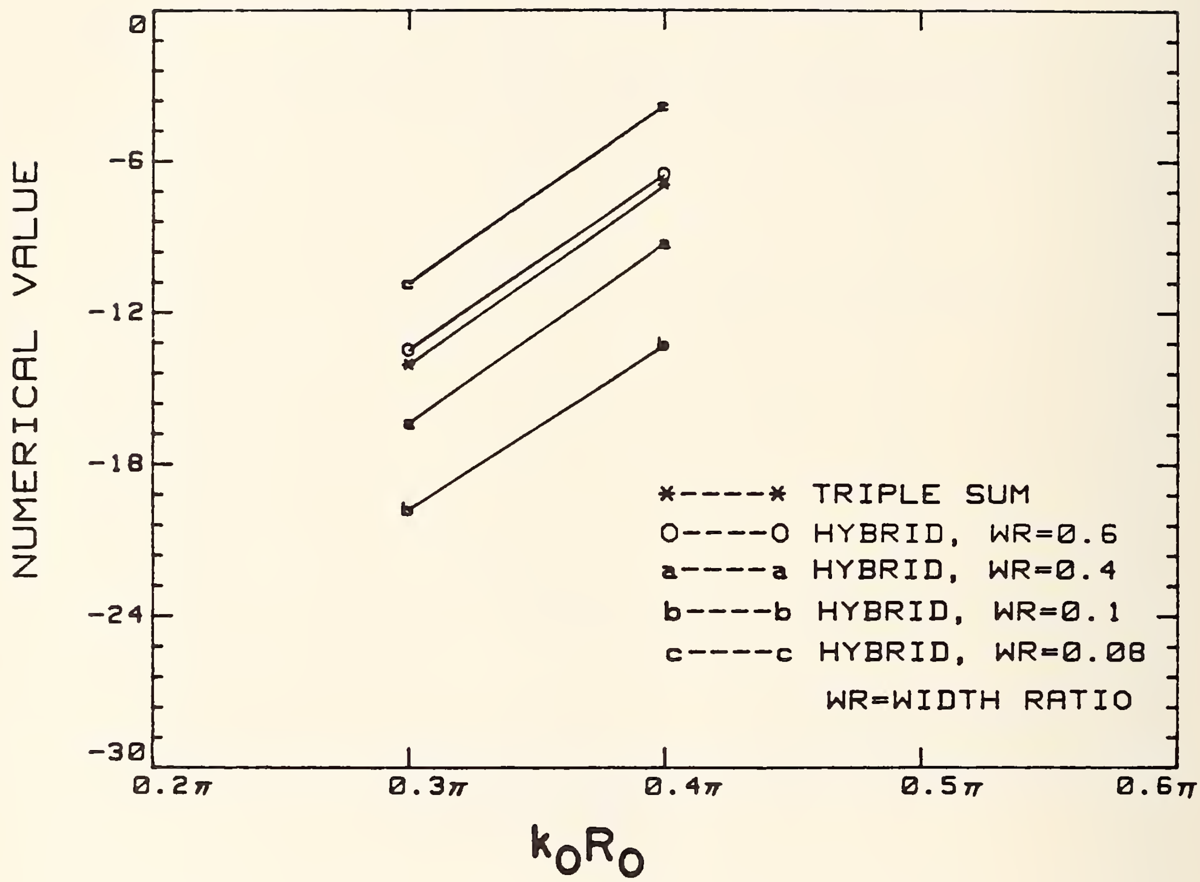


Figure 10: Comparison of the hybrid sum with G(r,r') for different width ratios.

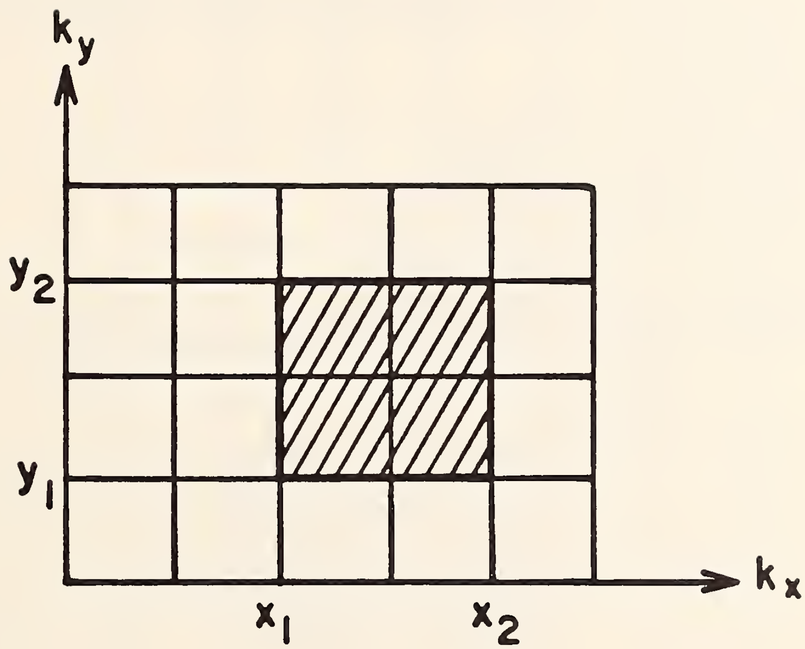


Figure A-1: A typical range of integration for the finite sum.

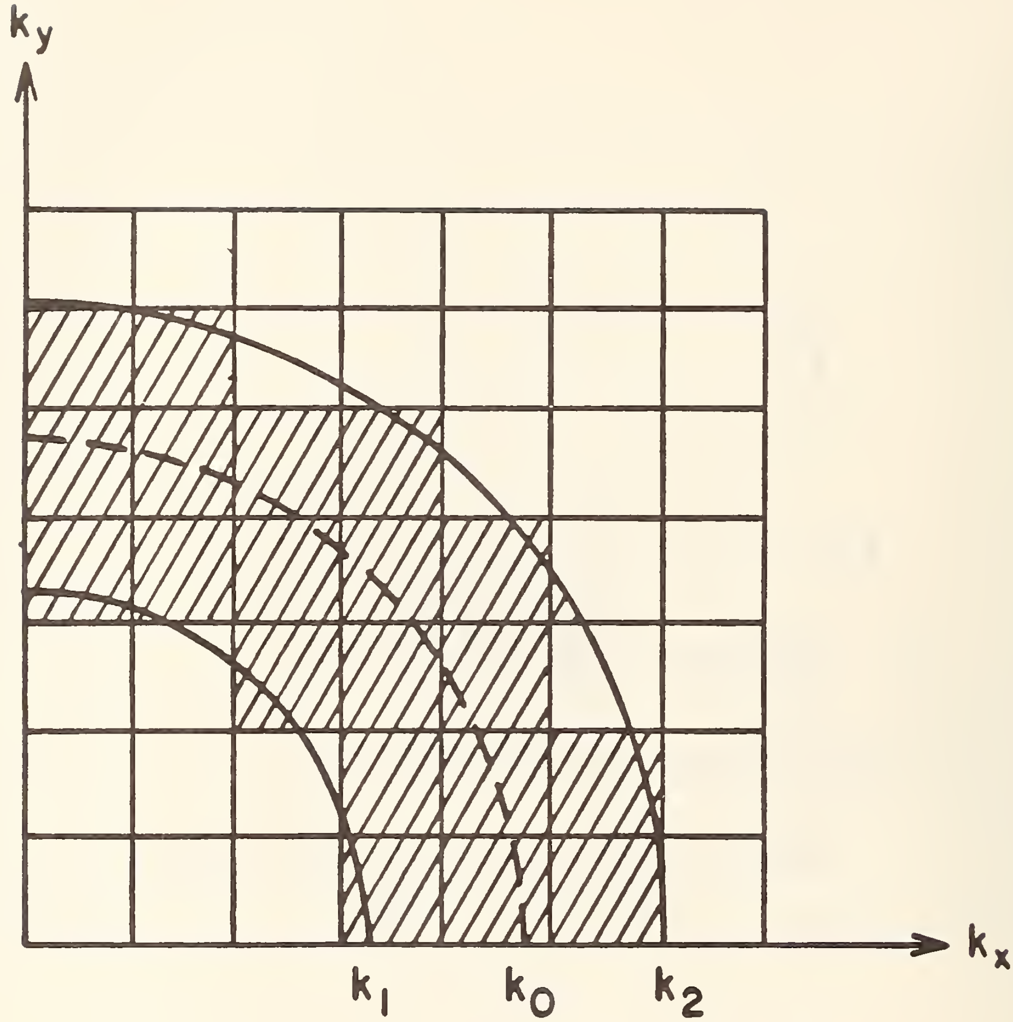


Figure A-2: Arrangement of a finite set of summation intervals.

NBS-114A (REV. 2-80)

| U.S. DEPT. OF COMM. BIBLIOGRAPHIC DATA SHEET (See instructions) | 1. PUBLICATION OR REPORT NO. NBS/TN-1312 | 2. Performing Organ. Report No. | 3. Publication Date September 1987 |
|---|---|---|---|

4. TITLE AND SUBTITLE

An Investigation of a Ray-Mode Representation of the Green's Function in a Rectangular Cavity

5. AUTHOR(S)

D. I. Wu and D. C. Chang

6. PERFORMING ORGANIZATION (If joint or other than NBS, see instructions)

NATIONAL BUREAU OF STANDARDS
DEPARTMENT OF COMMERCE
WASHINGTON, D.C. 20234

7. Contract/Grant No.

8. Type of Report & Period Covered

9. SPONSORING ORGANIZATION NAME AND COMPLETE ADDRESS (Street, City, State, ZIP)

10. SUPPLEMENTARY NOTES

[ ] Document describes a computer program; SF-185, FIPS Software Summary, is attached.

11. ABSTRACT (A 200-word or less factual summary of most significant information. If document includes a significant bibliography or literature survey, mention it here)

It is well known that a point-source excited field in a rectangular cavity can be represented either in terms of summation of modes or in terms of rays produced by the equivalent image sources. Both representations involve series that are slowly convergent, so computation of fields inside the cavity is difficult. To obtain a numerically efficient scheme, a hybrid ray-mode representation is developed here using the finite Poisson summation formula. The modal representation is modified in such a way that all the modes near resonance are retained while the truncated remainder of the mode series is expressed in terms of a weighted contribution of rays. For a large cavity, the contribution of rays from far away images becomes small, therefore the ray sum can be approximated by one or two dominant terms without a loss of numerical accuracy. To illustrate the accuracy and the computational simplification of this ray-mode representation, numerical examples are included with the conventional mode series (summed at the expense of long computation time) serving as a reference.

12. KEY WORDS (Six to twelve entries; alphabetical order; capitalize only proper names; and separate key words by semicolons)

Green's function; hybrid representation; modal representation; Poisson summation formula; ray-mode representation; rectangular cavity.

13. AVAILABILITY

[X] Unlimited
[ ] For Official Distribution. Do Not Release to NTIS
[X] Order From Superintendent of Documents, U.S. Government Printing Office, Washington, D.C. 20402.
[ ] Order From National Technical Information Service (NTIS), Springfield, VA. 22161

14. NO. OF PRINTED PAGES

48

15. Price

# *NBS* *Technical Publications*

## *Periodical*

**Journal of Research**—The Journal of Research of the National Bureau of Standards reports NBS research and development in those disciplines of the physical and engineering sciences in which the Bureau is active. These include physics, chemistry, engineering, mathematics, and computer sciences. Papers cover a broad range of subjects, with major emphasis on measurement methodology and the basic technology underlying standardization. Also included from time to time are survey articles on topics closely related to the Bureau's technical and scientific programs. Issued six times a year.

## *Nonperiodicals*

**Monographs**—Major contributions to the technical literature on various subjects related to the Bureau's scientific and technical activities.

**Handbooks**—Recommended codes of engineering and industrial practice (including safety codes) developed in cooperation with interested industries, professional organizations, and regulatory bodies.

**Special Publications**—Include proceedings of conferences sponsored by NBS, NBS annual reports, and other special publications appropriate to this grouping such as wall charts, pocket cards, and bibliographies.

**Applied Mathematics Series**—Mathematical tables, manuals, and studies of special interest to physicists, engineers, chemists, biologists, mathematicians, computer programmers, and others engaged in scientific and technical work.

**National Standard Reference Data Series**—Provides quantitative data on the physical and chemical properties of materials, compiled from the world's literature and critically evaluated. Developed under a worldwide program coordinated by NBS under the authority of the National Standard Data Act (Public Law 90-396). NOTE: The Journal of Physical and Chemical Reference Data (JPCRD) is published quarterly for NBS by the American Chemical Society (ACS) and the American Institute of Physics (AIP). Subscriptions, reprints, and supplements are available from ACS, 1155 Sixteenth St., NW, Washington, DC 20056.

**Building Science Series**—Disseminates technical information developed at the Bureau on building materials, components, systems, and whole structures. The series presents research results, test methods, and performance criteria related to the structural and environmental functions and the durability and safety characteristics of building elements and systems.

**Technical Notes**—Studies or reports which are complete in themselves but restrictive in their treatment of a subject. Analogous to monographs but not so comprehensive in scope or definitive in treatment of the subject area. Often serve as a vehicle for final reports of work performed at NBS under the sponsorship of other government agencies.

**Voluntary Product Standards**—Developed under procedures published by the Department of Commerce in Part 10, Title 15, of the Code of Federal Regulations. The standards establish nationally recognized requirements for products, and provide all concerned interests with a basis for common understanding of the characteristics of the products. NBS administers this program as a supplement to the activities of the private sector standardizing organizations.

**Consumer Information Series**—Practical information, based on NBS research and experience, covering areas of interest to the consumer. Easily understandable language and illustrations provide useful background knowledge for shopping in today's technological marketplace.

*Order the* **above** *NBS publications from: Superintendent of Documents, Government Printing Office, Washington, DC 20402.*

*Order the* **following** *NBS publications—FIPS and NBSIR's—from the National Technical Information Service, Springfield, VA 22161.*

**Federal Information Processing Standards Publications (FIPS PUB)**—Publications in this series collectively constitute the Federal Information Processing Standards Register. The Register serves as the official source of information in the Federal Government regarding standards issued by NBS pursuant to the Federal Property and Administrative Services Act of 1949 as amended, Public Law 89-306 (79 Stat. 1127), and as implemented by Executive Order 11717 (38 FR 12315, dated May 11, 1973) and Part 6 of Title 15 CFR (Code of Federal Regulations).

**NBS Interagency Reports (NBSIR)**—A special series of interim or final reports on work performed by NBS for outside sponsors (both government and non-government). In general, initial distribution is handled by the sponsor; public distribution is by the National Technical Information Service, Springfield, VA 22161, in paper copy or microfiche form.

**U.S. Department of Commerce**
National Bureau of Standards
Gaithersburg, MD 20899